Thermal Science and Engineering Progress 37 (2023) 101534

Contents lists available at ScienceDirect

Thermal Science and Engineering Progress

journal homepage: www.sciencedirect.com/journal/thermal-science-and-engineering-progress

Performance improvement potential of a PV/T integrated dual-source heat pump unit with a pressure booster ejector

M. Tahir Erdinc [a], Cagri Kutlu [b,*], Saban Unal [c], Orhan Aydin [d], Yuehong Su [b,*], Saffa Riffat [b]

[a] Department of Mechanical Engineering, Tarsus University, 33400 Tarsus/Mersin, Turkey
[b] Department of Architecture and Built Environment, Faculty of Engineering, University of Nottingham, NG7 2RD, UK
[c] Department of Mechanical Engineering, Osmaniye Korkut Ata University, 80000 Osmaniye, Turkey
[d] Department of Mechanical Engineering, Karadeniz Technical University, 61080 Trabzon, Turkey

ARTICLE INFO

Keywords:
Dual-source
Ejector
PV/T
Heat pump
COP improvement

ABSTRACT

Dual-source heat pump unit can utilize the evaporation of the refrigerant at two different pressures. By adopting an ejector, high-pressure refrigerant stream can be used to lift compressor inlet pressure which results in a higher coefficient of performance (COP). This study proposes a renewable energy sourced and high-efficiency heat pump system which can be easily building integrated to offer a renewable heating solution. The system is devised on the complementation of dual thermal sources; one is air and the other one is solar, to maximize the utilization of ambient energy for highly efficient operation of heat pump. Using the advantage of the relatively lower operating temperature in the solar collector line, the thermal efficiency of the collector would be sufficient in winter. Adaptation of photovoltaics in the collector as a PV/T unit, will benefit the system from the produced electricity for further reduction of the demand from the grid. Along with the use of PV/T collector, the system can be potentially carbon neutral for larger collector areas. In this study, the performance improvement potential of a dual-sourced heat pump unit with an ejector as a booster is investigated for different locations in Turkey which presents different solar and weather profiles. The optimum collector evaporation temperatures are determined, and COP improvement potentials are discussed for different conditions. For a heating supply of 5 kW, the COP of the system can be improved by 22.6 % under 400 W/m^2 and 10 °C ambient using 15 m^2 PV/T collector. Including the electricity generated from the PV, reduction of the electricity demand from the grid can reach to 75 % for the same conditions.

1. Introduction

To tackle the challenge of growing energy demand of countries, energy efficiency and renewable energy are the most important components of energy strategy. Among different sectors, energy demand of buildings has increased, significantly. More than half of the energy demand in dwellings is associated with space and water heating, therefore efficiency improvement and utilisation of renewable energy in space and water heating could make a significant contribution [1].

Heat pump technology is an attractive option for heating dwellings because of its low electricity consumption compared to electrical heaters [2]. It is also an environmentally friendly system with zero direct carbon release against boiler systems. Developing an energy-efficient and environmentally friendly heat pump system which shows the potential of improving people's residential thermal environment and mitigates the challenges in energy and environment is very important. However, grid electricity consumption also causes carbon emissions because of carbon-based fuel burning for electricity generation.

Conventional and commonly used heat pumps are air-source heat pumps which are easy to install and versatile for buildings [3]. Researchers have studied on combination of heat pump system with solar system to enhance performance of the heat pump [2]. Therefore, solar-assisted heat pump (SAHP) system has been developed to elevate the evaporation temperature and to reach a higher COP than the air-source heat pump [4]. A comprehensive review on solar assisted heat pump technology was done by Buker and Riffat [5], and they presented that this combination could be a good method to reduce fossil fuel consumption. In solar assisted heat pump systems, solar energy is absorbed by the refrigerant and takes this energy to the system. Also, on the solar side, since the solar collector (evaporator) refrigerant evaporates at lower temperature, the energy conversion by the collector enhances [6].

* Corresponding authors.
E-mail addresses: cagri.kutlu2@nottingham.ac.uk (C. Kutlu), yuehong.su@nottingham.ac.uk (Y. Su).

https://doi.org/10.1016/j.tsep.2022.101534
Received 3 August 2022; Received in revised form 29 October 2022; Accepted 30 October 2022
Available online 4 November 2022

Nomenclature

A_{col}	collector area [m^2]
$COP_{HP,ej}$	coefficient of performance of ejector enhanced heat pump [-]
$COP_{HP,conv}$	coefficient of performance of the conventional heat pump [-]
G	solar irradiance [W/m^2]
h	enthalpy [J kg^{-1}]
$\dot{m}$	mass flow rate [kg s^{-1}]
P	pressure [Nm^{-2}]
R_{grid}	reduction from grid [%]
$\dot{Q}_{con}$	heating capacity of condenser [W]
$\dot{Q}_{solar}$	solar heat input [W]
s	entropy [J $kg^{-1}K^{-1}$]
T	temperature [°C]
x	quality [-]
x_{cover}	cover ratio [-]
u	velocity [m/s]
$\dot{W}_{comp}$	compressor work [W]
$\dot{M}^*$	entrainment ratio [-]

Greek symbols

ΔT_{sh}	superheating temperature difference [°C]
ΔT_{sc}	subcooling temperature difference [°C]
η_c	isentropic efficiency of compressor [-]
η_{gen}	generator efficiency [-]
η_{mec}	mechanical efficiency of compressor [-]
η_n	isentropic efficiency of nozzle [-]
η_d	isentropic efficiency of diffuser [-]
η_m	mixing section efficiency [-]
η_{PV}	PV efficiency

Subscripts

am	ambient
col	collector
con	condenser
conv	conventional
dis	discharge
ej	ejector
gen	generator
HP	heat pump
m	mean
suc	suction
th	thermal

Kong et al. [7] experimentally investigated a domestic hot water supply system with a direct-expansion solar assisted heat pump unit for different parameters, and their results showed that higher solar radiation increases the COP of the unit.

In practical applications, single source or one evaporator is faced with different problems such as limited heating capacity. Thus, the researchers interested in dual source heat pump systems which the cold source is aided by another source like ground source or solar collector and this additional source can be in series or dual for the multi-source heat pump system [8]. During the day time, two different evaporator temperatures, one absorbs heat from solar energy and the other uses outside air, so that heating capacity and the COP can be increased [9]. Various studies were carried out on dual source heat pump systems have been performed by researchers [10–13]. Grossi [14] investigated annual and seasonal energy performance of dual source heat pump unit using air and ground source. Han et al. [15] conducted experiments for the double source heat-pipe composite vapor compression heat pump. They stated that COP of the heating unit could be improved under heat pipe operating condition by 27.61 % and 27.85 %, and by 5.14 % and 4.90 % under vapour compression operating condition. Liu et al. [16] developed three different working modes of solar air composite heat source heat pump system. Their experimental results showed that the usage of this composite system could enhance the performance of the heat pump by increasing 51 % in heat capacity and 49 % in COP. Cai et al. [17] experimentally and numerically investigated the multi-functional heat pump with solar-air composite source. They mentioned that as the solar radiation intensity increases, solar collector capacity increases, but change of evaporation capacity of air evaporator shows opposite trend. Liu et al. [18] conducted a simulation for different refrigerant flow rates and distributions of dual source solar-air heat pump system. They established a dynamic simulation model by TRNSYS and validated their results with experimental data. They suggested that solar collector and evaporator refrigerant flow ratio should be appropriate to improve performance of the heat pump.

Moreover, photovoltaic thermal (PV/T) collector can be integrated into the heat pump system to benefit electricity generation. Pei et al. [6,19] studied PV/T collector in their system, and presented that some portion of the solar energy was converted to electricity and the remaining part was taken as heat for evaporation. As a result of lower PV cell temperature and absorption of solar energy, PV efficiency and COP could be improved. Cai et al. [20] presented a dynamic simulation and performance characterization of PV/*T*-air dual source heat pump water heater system. They pointed out that when the solar irradiance increases from 100 W/m^2 to 300 W/m^2 COP of the system be increased from 2.21 to 2.39. Du et al. [9] experimentally investigated the electrical and thermal performance of heat-collecting evaporator and PV/T air dual source direct-expansion heat pump. They compared three modes under winter typical heating conditions.

Another method to increase COP of the vapour compression systems is to use an ejector to reduce expansion losses. The conventional air source heat pumps, regardless of whether they are solar-assisted or not, use a capillary tube or a throttle valve to expand the working fluid and, this process causes to thermodynamic loss called throttling loss where expansion energy is entirely dissipated through friction [21]. Therefore, an opportunity is presented to improve the COP of the air source heat pump by introducing an ejector as an expansion energy recovery devices, which leads to ejector-expansion heat pump technology [22].

The usage of ejector in refrigeration and heat pump systems are given in many studies [23–28]. A detailed review on the usage of ejector in refrigeration and solar powered refrigeration systems was conducted by Besagni et al. [27]. Focusing on the past, present, and future trends, the technology of ejector and its behaviour, properties of the refrigerant and their influence on the ejector performance and ejector refrigeration systems were presented. Lin et al. [29] conducted experiments for a multi evaporator refrigeration system and their results showed that pressure recovery ratio could be increased up to 20 %. In heat pump systems, many studies were conducted related to solar driven/enhanced ejector systems [30–33]. Liu and Lin [34] used zeotropic mixture R1270/R600a and analysed a dual-temperature air source heat pump with ejector enhanced system. Their results showed COP, heating capacity per volume and the second law efficiency were improved by 36.5 %, 37.2 and 38.5 %, respectively. The same authors [35] used R1234yf, R290 and R134a as working fluid and conducted thermo-economic performance of the dual temperature air source ejector heat pump system. It was shown that the system with an ejector significantly outperformed the system without ejector in terms of exergy efficiency, exergy destruction and economy. Wang et al. [36] studied a dual temperature air source ejector enhanced heat pump system based on energy

and exergy analysis. Compared to the conventional heat pump system, their configuration had improvements; 24.93 % on COP, on the 24.92 % volumetric heating capacity and on the 38.84 % exergetic efficiency.

Chen and Yu [22] studied a water heater direct expansion solar assisted ejector-compression heat pump system for two different operation modes. Simulation results showed that COP could be increased by 13.78 and 25.07 %. As a water heater, Fan et al. [31] analysed a modified ejector-compression heat pump system using zeotropic mixture R290/R600a. They stated that glide property of the zeotropic mixture had a better matching characteristic. Zhu et al. [37] analysed the a performance of a dual-nozzle ejector enhanced for solar assisted air-source heat pump system. They stated that, for given operating conditions the COP value was enhanced by 4.6–34.03 % compared to the conventional ejector enhanced heat pump systems.

It is known that the role of the ejector geometry plays a very important role for the optimum performance of the system and this optimum performance is affected by the operating conditions [38]. For the steam-jet ejector, Sun [38] studied variable ejector geometry to see the effect of the ejector geometry on system performance, flow rates and entrainment ratio. It was shown that entrainment ratio and the COP of the system suddenly dropped and reached to zero when the back pressure was higher than a critical value. The utilization of variable primary nozzle geometry was numerically investigated for R600a and R152a refrigerants by Varga et al. [39]. Using a moveable spindle at the nozzle to make variable area ratio, they found that when the operating conditions are different from the design condition the variable nozzle could enhance the entrainment ratio and ejector performance by 177 %. Li et al. [40] presented performance of the variable ejector for multi evaporator refrigeration system. They mentioned that the pressure recovery ratio, critical area ratio and the entrainment ratio were highly affected by the secondary and primary pressures. An experimental study conducted by Li et al. [41] showed that energy efficiency of the multi-evaporator refrigeration system could be enhanced by 12 % using the variable area ratio ejector. Li et al. [42] numerically investigated the effects of area ratio, nozzle exit position (NXP), primary nozzle length and diffuser length on the entrainment ratio. They found that the entrainment ratio was highly influenced by the area ratio and NXP.

According to the literature review given above, using a dual-source heat pump and an ejector both results in a positive effect on COP improvement separately. Although the dual-source heat pump studies investigated the collector efficiency, ejector heat pump studies were mostly conducted as parametric studies. In addition, collector efficiency should be taken into consideration to reflect real operation conditions because evaporation temperature of the high-temperature evaporator, which is PV/T collector evaporation temperature in this study, affects both ejector performance and collector efficiency. It is necessary to optimize solar collector temperature to maximize the benefit from the dual-source heat pump, ejector, and the PV/T performance. In this study, condenser exit splits into two ways, one stream enters to PV/T collector, and the another enters to the low-temperature evaporator without adapting a separator or heat exchangers. In these two lines, evaporation pressures and mass flow rates can be controlled by expansion valves. With this configuration, the system can operate more efficiently by taking advantage of optimum ejector and solar collector responses. This article investigates optimum operating temperatures for different weather conditions. After determination of the best operation conditions, COP improvement potential and reduction of demand from the grid are simulated for one month for two different locations to present performance under different weather conditions.

2. System description

In this study, an ejector enhanced solar-assisted and air source heat pump system integrates the benefits derived from the solar source and ejector to improve the system performance. Fig. 1a shows the schematic view of the system. The PV/T collectors are employed as assisting units to provide both heat and electricity to the system. The gained heat can boost the ejector performance and compressor inlet pressure. Moreover, the generated electricity can reduce electricity demand from the grid.

As shown in Fig. 1, the proposed system utilizes dual evaporators (one is an air source and the other one is a solar source) with an ejector to reduce the electricity consumption on the compressor by decreasing the compression pressure ratio. The working principle of the system can be explained by using pressure enthalpy diagram which is given in Fig. 1b, as follows: At the condenser outlet (state 3), the refrigerant is split into two lines; the first line for solar PV/T collector, and another line for air source heat exchanger. The required pressures are adjusted according to conditions (solar irradiance intensity and ambient temperature) by expansion valves. The refrigerant at collector line (high pressure) initially goes into an expansion valve where its temperature drops to the collector temperature (state 4). Later the refrigerant enters the solar collector and evaporates (state 5). The pressure of the refrigerant at air source heat exchanger line (low pressure) decreases in the expansion valve (state 7) and evaporates by the air source heat exchanger (state 8). The ejector uses the high-pressure refrigerant as a driving mainstream and lifts the pressure of the low-pressure refrigerant (states 6 and 9). As a result, the compressor power is reduced, and heat pump performance is improved. As the electricity generated by the PV/T collector reduces the grid electricity demand, it will be further downscaled.

3. Modelling of the system components

The proposed unit consists of a compressor, a condenser (split unit at the room), two expansion valves, a PV/T evaporator, an ejector, and an air sourced evaporator. In order to present the performance improvement potential of the unit, the modelling part is simplified. The following assumptions are considered for the heat pump simulation:

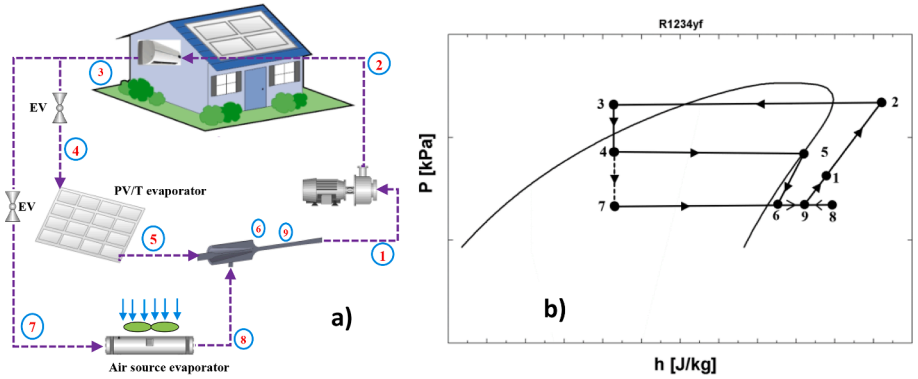

Fig. 1. a) Schematic view of the solar-air dual source heat pump with use of pressure booster ejector, **b)** Pressure-Enthalpy diagram of the system.

- The condensation and evaporation processes in the condenser and evaporator are assumed to be at constant pressures.
- The evaporation temperature in the air source evaporator is assumed as 10 °C lower than the ambient temperature. However, condensation temperature is fixed at 40 °C.
- An isenthalpic expansion occurs in the expansion valves.
- The refrigerant exits from the solar PV/T evaporator as saturated vapor.
- The subcooling and superheating temperatures are assumed as 5 °C.

The compressor power consumption changes with operating conditions. The compressor power consumptions of the conventional air sourced heat pump and the ejector enhanced dual source heat pump are determined as follows:

$$\dot{W}_{comp,conv} = \dot{m}_{r,conv} \bullet (h_2 - h_8) \Big/ \eta_{mec} \tag{1}$$

$$\dot{W}_{comp,ej} = \dot{m}_{r,ej} \bullet (h_2 - h_1) \Big/ \eta_{mec} \tag{2}$$

where; η_{mec} is the mechanical efficiency of the compressor, which is taken 0.95 [43] and isentropic efficiency of the compressor is calculated from [44]:

$$\eta_{is} = 0.874 - 0.0135 \bullet \frac{P_{dis}}{P_{suc}} \tag{3}$$

The COPs of the heat pump and ejector enhanced heat pump are defined as follows:

$$\mathrm{COP}_{HP,\,conv} = \frac{\dot{Q}_{con}}{\dot{W}_{comp,conv}} \tag{4}$$

$$\mathrm{COP}_{HP,\,ej} = \frac{\dot{Q}_{con}}{\dot{W}_{comp,ej}} \tag{5}$$

where $\dot{Q}_{con}$ is condenser heating capacity which equals to supplied heat to the building.

3.1. PV/T collector model

In operation, the PV/T collector is a heat exchanger of the high temperature evaporation line. The refrigerant flows through the collector and completely evaporates at designed or determined temperature and pressure. As the operation temperature will be lower than the condensation temperature, a conventional PV/T flat plate collector can show a proper performance. Therefore, the flat plate PV/T collector thermal and electrical efficiency equations for the are used in the calculations and validated equations are taken from Bhattarai et al. [45]. It is reported that the thermal efficiency of the direct steam generation collectors is higher than the one-phase working mode because of better heat transfer coefficient from fluid to collector tube [46], however, a conservative approach has been followed in this study to show potential improvement Eq. (6) gives the solar heat input to the system and Eq. (7) can be used for the collector thermal efficiency.

$$\dot{Q}_{solar} = A_{col} \bullet G \bullet \eta_{th} \tag{6}$$

$$\eta_{th} = 0.574 - 7.41 \bullet \frac{(T_m - T_{am})}{G} - 0.0023 \bullet \frac{(T_m - T_{am})^2}{G} \tag{7}$$

where A_{col}, G and T_{am} are the collector area, the solar radiation, and the ambient temperature, respectively. T_m indicates the mean temperature of the working fluid, however in this study, the refrigerant evaporates in the collector at constant temperature. Thus, T_m will be the evaporation temperature in the PV/T collector in the modelling.

For the electrical output of the collector, the following equations can be used:

$$\dot{W}_{PV} = A_{col} \bullet G \bullet \eta_{PV} \bullet x_{cover} \bullet \eta_{gen} \tag{8}$$

$$\eta_{PV} = 0.1369 - 0.477 \bullet \frac{(T_m - T_{am})}{G} \tag{9}$$

where x_{cover} and η_{gen} are the PV cover ratio and the generator efficiency which are taken 0.8 and 0.9, respectively.

The reduction from the grid is an important parameter when a PV/T module is used. R_{grid} is defined as given:

$$R_{grid} = \frac{\dot{W}_{comp,conv} - \left(\dot{W}_{comp,ej} - \dot{W}_{PV}\right)}{\dot{W}_{comp,conv}} \times 100\% \tag{10}$$

3.2. Ejector modelling

The flow in the ejector can be one or two phase according to operating conditions. Each state in the ejector is illustrated in Fig. 2. As shown in Fig. 2, the ejector has three main parts: namely, the nozzle, the mixing region, and the diffuser. The high temperature and pressure refrigerant leaving the collector enters the nozzle (state 5) and mixed with the refrigerant coming from the low temperature evaporator in the mixing region. Then, pressure of the refrigerant increases along the diffuser section and enters the compressor (state 1) with a pressure which is greater than the low temperature evaporator pressure. The ejector equations are taken from reference Unal and Yilmaz [47].

State 6 can be found using isentropic efficiency of the nozzle definition:

$$\eta_n = \frac{h_5 - h_6}{h_5 - h_{6s}} \tag{11}$$

where state 5 is the high temperature evaporator (collector) exit and state 6 is the low temperature evaporator exit. h_{6s} can be found using the following relations:

$$s_{6s} = s_5 \tag{12}$$

$$s_5 = f(P = P_5, x_5 = 1) \tag{13}$$

$$h_{6s} = f(P = P_{6s}, s = s_{6s}) \tag{14}$$

The pressure at the exit of the nozzle is assumed to be equal to the low temperature evaporator pressure.

$$P_{6s} = P_8 \tag{15}$$

Applying the energy equation between state 5 and 6, the velocity at the exit of the nozzle (state 6) can be determined as follows:

$$u_6 = (2 \bullet (h_5 - h_6))^{0.5} \tag{16}$$

The energy equation in the mixing region can be written as:

$$h_6 + \frac{u_6^2}{2} + \dot{M}^* \bullet h_8 = (1 + \dot{M}^*) \bullet \left(h_9 + \frac{u_9^2}{2}\right) \tag{17}$$

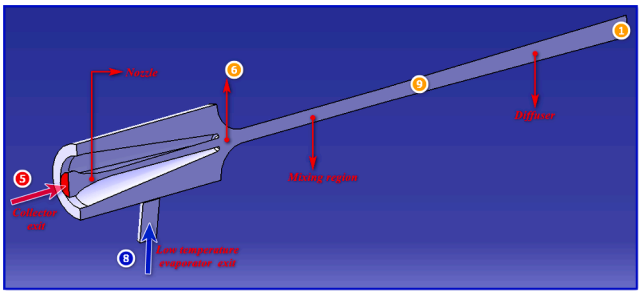

Fig. 2. The details of the ejector.

Here, state 9 is the exit of the mixing region. Utilizing mixing efficiency (η_m), the velocity of the state 9 can be determined as:

$$u_9 = u_6 \bullet \left(\frac{\eta_m}{1+\dot{M}^*}\right)^{0.5} \quad (18)$$

η_m takes the frictional losses into consideration [47]. The entrainment ratio $\dot{M}^*$ is defined as follows:

$$\dot{M}^* = \dot{m}_8/\dot{m}_5 \quad (19)$$

where $\dot{m}_5$ and $\dot{m}_8$ are the mass flow rates of the refrigerant coming from the collector and low temperature evaporator, respectively.

The diffuser exit (state 1) can be determined as:

$$h_1 = h_9 + u_9^2/2 \quad (20)$$

$$h_1 = h_9 + \frac{(h_{1s} - h_9)}{\eta_d} \quad (21)$$

where η_d is diffuser efficiency and the entropy values are found with the following relations:

$$s_{1s} = s_9 \quad (22)$$

$$s_9 = f(h_9, P_9) \quad (23)$$

4. Results

4.1. Design conditions

Design parameters of the system are determined in this section. The proposed unit is a heat pump, and it operates in winter condition. Since this study aims to present the advantages of combining solar and air sources, the analysis is based on assuming a constant heating output, but the weather conditions are changed. The weather data were chosen to cover different locations in Turkey. As a weather reference, the coldest months of Adana (latitude 37.00167, longitude 35.32889) and Istanbul (latitude 41.0082, longitude 28.9784) cities were taken. Fig. 3 shows solar radiation and ambient temperature variation during the coldest months. The data are taken from EnergyPlus weather data [48]. As

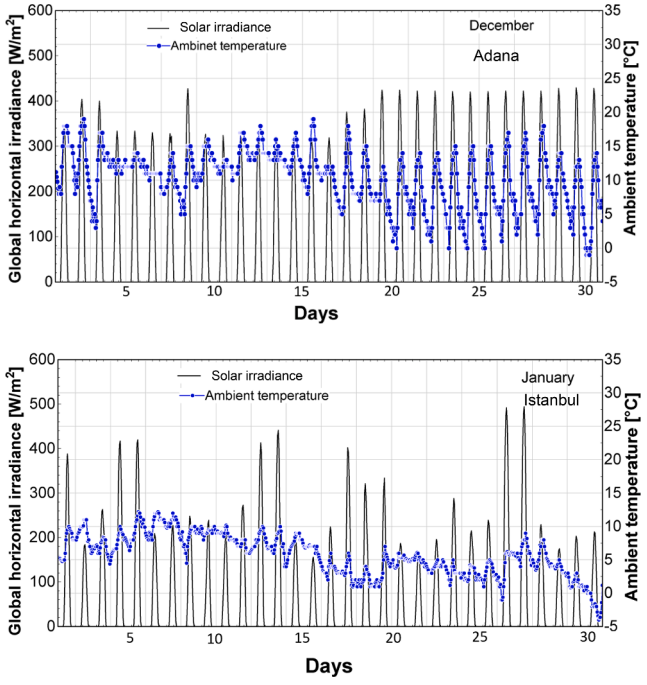

Fig. 3. Typical winter weather profiles of Adana and Istanbul, Turkey.

winter conditions, the global solar irradiance reaches maximum 460 W/m^2 and ambient temperature varies between 19 °C to −3°C, however, the hours of under zero-degree temperatures are limited, which occur at night. As a design condition, the ambient temperature is chosen as 5 °C to cover coldest conditions but the performance of the unit will be investigated for different ambient temperatures in this parametric study.

The condensation temperature is fixed at 40 °C as a space heating requirement and designed heating capacity of the heat pump is 5 kW. A solar collector area of 15 m^2 is chosen, which can be suitable for most of the houses. The designed solar irradiance is chosen as 200 W/m^2. By using the given conditions, the evaporation temperature of the PV/T collector (refrigerant temperature in the collector line) is calculated as 7 °C for a solar input of 1.5 kW. A low global warming refrigerant, R1234yf, is also adopted to the heat pump unit. The summary of design parameters is given in Table 1.

By using design conditions, pressure enthalpy diagram is formed (Fig. 4). This condition was chosen for a conservative approach in order to reflect the worst operation condition in winter. State 5 indicates collector output and entrance to the ejector. The ejector operates in one phase. After the nozzle in the ejector (state 6), the collector flow is mixed with the refrigerant which comes from the air evaporator (state 8). The mixture (state 9) enters to the diffuser and its pressure is increased to state 1. As the pressure lift is low in this condition, COP improvement is calculated as 7.6 %. However, operation conditions are changed during the day and COP improvement will be investigated in following sections.

4.2. Impact of PV/T evaporator temperature for a constant solar heat input

The refrigerant temperature flowing in the collector is referred to as the temperature of the PV/T evaporator temperature, because the refrigerant phase is changed from liquid to vapour at a constant temperature. This section investigates the effect of collector evaporation temperature for a constant solar input since the pressure lift is significantly affected by the collector evaporation temperature and pressure. The effect of the PV/T evaporator temperature on the pressure lift and COP improvement are illustrated in Fig. 5. From this figure, pressure at the compressor inlet could be increased from 277 kPa to 303.7 kPa with an increase of the collector evaporation temperature from 0 °C to 13 °C. For lower collector evaporation temperatures, COP improvement would decrease and fall to zero at −5°C. The pressure lift can enhance the COP up to 11.3 %. However, it should be noted that this figure is plotted for a constant solar input which means higher collector temperatures will have lower flow rates as the latent heat is larger for the higher PV/T evaporation temperature, (see the P-h diagram in Fig. 4) as constant solar heat input is considered in this figure. Thus, Fig. 6 is given for mass flow rates on the air evaporator and collector lines. The mass flow rates are slightly affected by the PV/T evaporation temperature. Since the mass flowrate in the collector decreases and air source evaporator mass flowrate increases with collector temperature, the higher collector temperature results in better entrainment ratio because driving stream pressure increases.

It is drawn from literature studies that the ejector geometry has an important effect on the entrainment ratio and system COP for variable

Table 1
Design parameters of the dual source heat pump unit.

Condensation Temperature	40 °C
Ambient temperature	5 °C
Air source evaporator pinch temperature difference	10 °C
Heating capacity of heat pump	5 kW
Collector area	15 m^2
Solar irradiance	200 W/m^2
Solar heat input to the system	1.5 kW
Evaporation temperature of PV/T evaporator	7 °C
PV electricity conversion efficiency	13.21 %

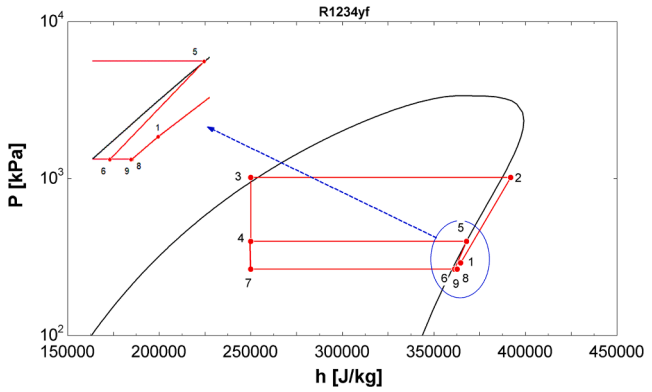

Fig. 4. P-h diagram of the dual-source heat pump under design conditions.

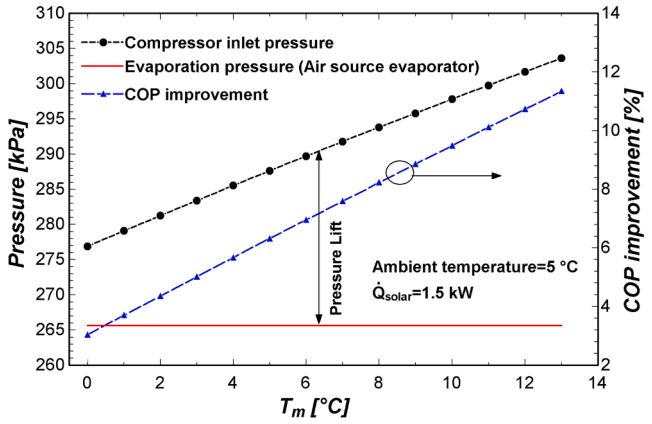

Fig. 5. Effect of PV/T collector evaporation temperature (T_m) on pressure lift and COP improvement.

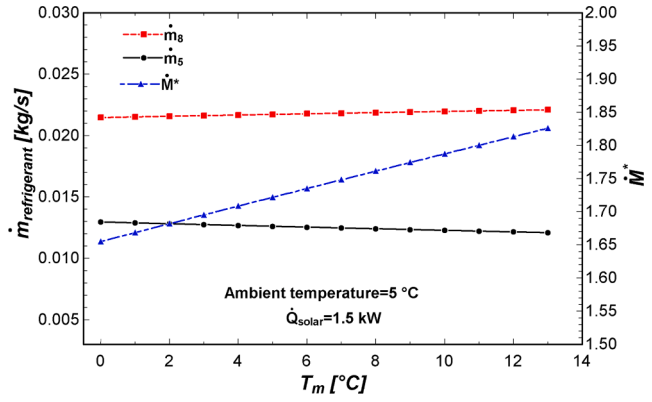

Fig. 6. Effect of PV/T collector evaporation temperature on refrigerant mass flow rates of air source evaporator ($\dot{m}_8$) and PV/T collector ($\dot{m}_5$) and entrainment ratio.

operating conditions [39–41,49–52]. Thus, variable operation conditions can be operated by the adjustable ejector for further studies.

4.3. The impact of solar irradiance

Solar irradiance is the key parameter for the system performance as it is directly related to solar input and the PV output. The performance improvement can be in two ways: Higher solar input has a positive effect on the ejector performance which increases mass flow rate in the PV/T evaporator line for the same evaporation temperature or increases the evaporation temperature (pressure) that results in a better ejector performance. Additionally, higher solar irradiance increases the PV output. In Fig. 7a, the variation of the collector thermal efficiency (Eq. (8)) with collector temperature for different solar irradiances is presented. As expected, thermal efficiency increases with the solar intensity, and it is high for lower collector evaporation temperatures. The solar collector heat input (Eq. (6)) variation is given in Fig. 7b.

Based on the PV/T collector efficiency calculations, the effect of the PV/T evaporator temperature on the COP improvement compared to air source heat pump operation is illustrated in Fig. 8. The PV/T evaporator temperature has a positive impact on COP improvement until a certain point. After that point, this improvement decreases. This negative effect is a reason of decreasing collector thermal efficiency by collector temperature as can be seen in Fig. 7a. Moreover, Fig. 8a shows the COP improvement, and the optimum collector temperature increase with the solar intensity. This optimum collector operation temperature changes almost linearly with higher solar radiation. When the ambient temperature is 5 °C, the maximum COP improvement by 5.4 % under 150 W/m^2 irradiance, improves by 21 % under 400 W/m^2. In addition to the COP improvement, the other advantage of the proposed system is a reduction of the demand from the grid shown in Fig. 8b. While the solar irradiance increases, the generated electricity from the PV cells also increases. By this way, the demand from the grid reduces. However, increasing the PV/T evaporator temperature negatively affects the PV efficiency and the reduction of demand from the grid.

Changing the ambient temperature from 5 °C to 10 °C, effect of the PV/T evaporator temperature and solar irradiance on COP improvement is depicted in Fig. 9. Similar trends are seen from the figure as optimum temperature increases with PV/T evaporator temperature and COP

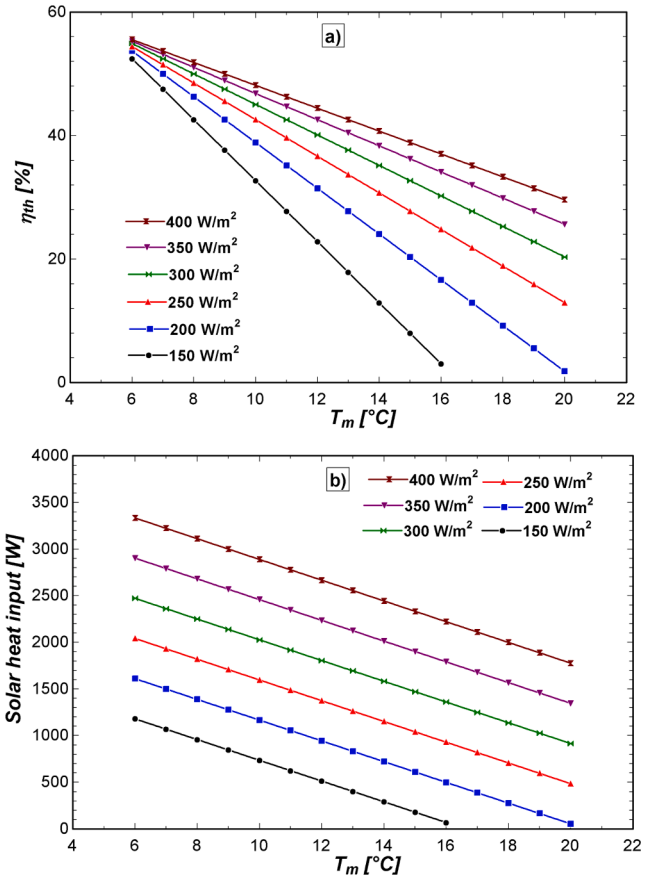

Fig. 7. (a) The change of PV/T collector thermal efficiency with solar collector performance with solar radiation and collector temperature **(b)** The change of solar heat input with solar radiation and collector temperature.

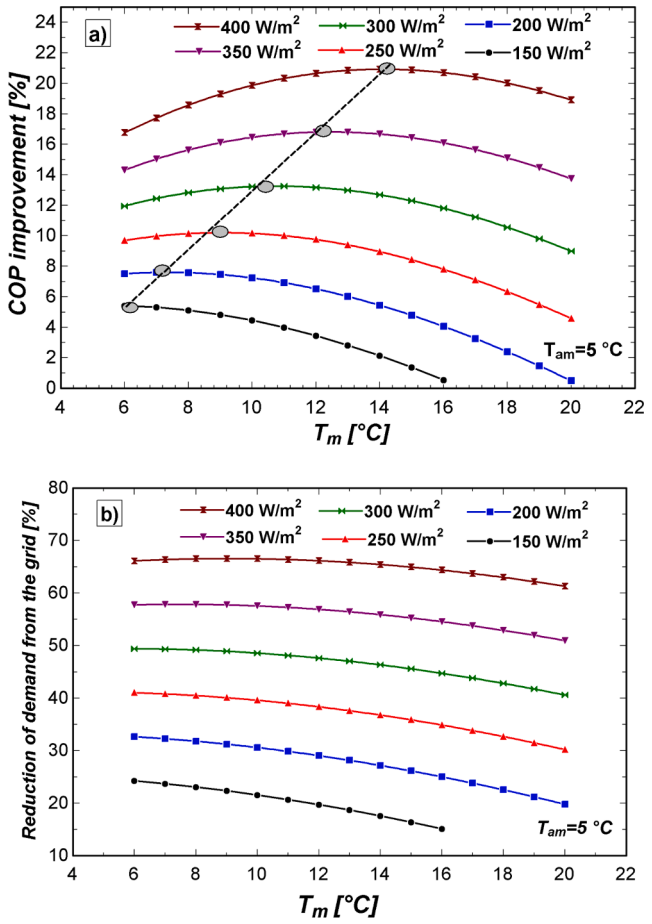

Fig. 8. a) COP improvement without PV contribution by PV/T collector evaporation temperature and solar irradiance (T_{am} = 5 °C) b) Reduction of demand from the grid with PV contribution.

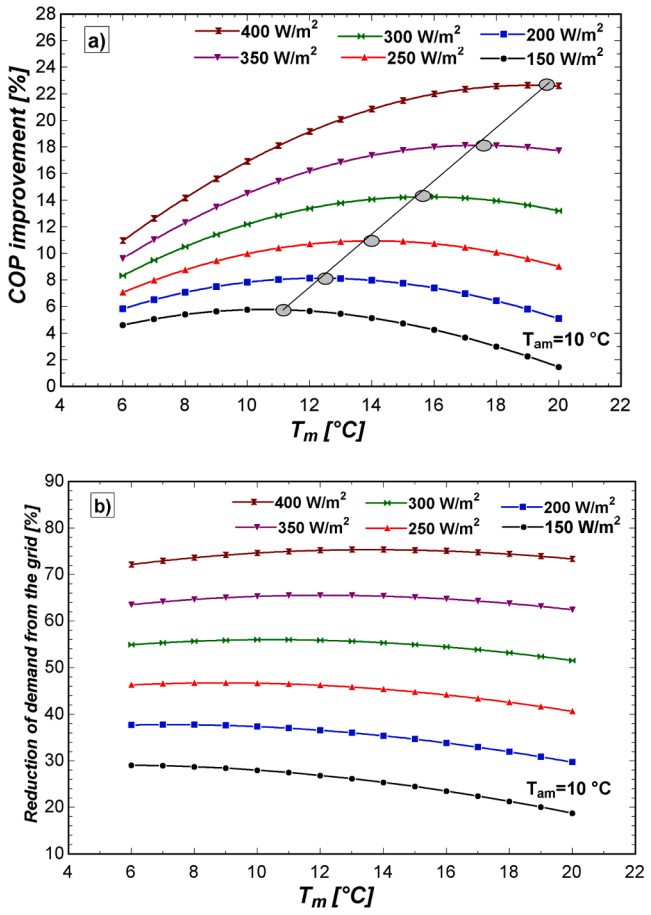

Fig. 9. a) COP improvement without PV contribution by PV/T collector evaporation temperature and solar irradiance (T_{am} = 10 °C) b) Reduction of demand from the grid with PV contribution.

improvement increases with solar irradiance. However, the optimum collector temperatures increase with increasing ambient temperature and the maximum COP increment reaches 22.6 %, and reduction of demand from the grid reaches 75 % under 400 W/m^2 solar irradiance.

4.4. The impact of ambient temperature

The previous section investigates the impact of solar irradiance, and it showed that ambient temperature is also an important parameter for the system performance. Because outside temperature influences the air source evaporator evaporation temperature and the PV/T thermal efficiency. Fig. 10 shows the effect of the PV/T collector evaporation temperature on COP improvement for various ambient temperatures at solar irradiance of 300 W/m^2. The optimum collector temperature is also strongly sensitive to the ambient temperature with an increasing trend as shown in the figure. The maximum COP improvement is also increased approximately from 12.5 % to 17.5 % when the ambient temperature increases from 0 °C to 20 °C. Therefore, the effect of the ambient temperature is investigated by using optimum PV/T collector evaporation temperatures for the solar irradiances considered.

Fig. 11 shows effect of ambient temperature on the COP improvement for different solar irradiance values when optimum PV/T evaporator temperatures are used. It is shown that the effect of ambient temperature slightly increases the COP improvements because conventional heat pump COP also increases with ambient temperature. However, this effect becomes more dominant under higher solar irradiances.

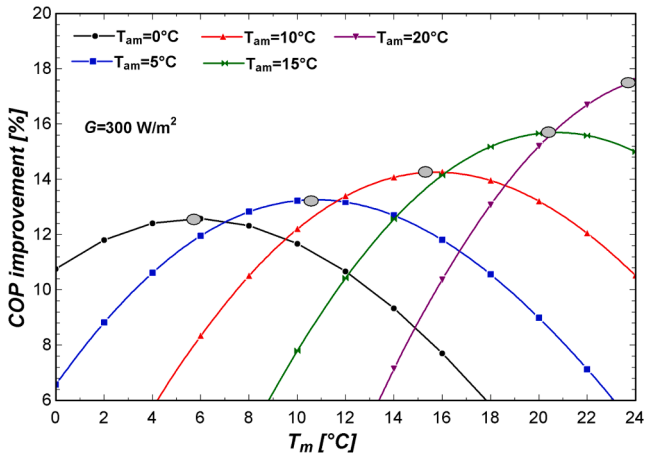

Fig. 10. COP improvement with PV/T collector evaporation temperature for different ambient temperatures ($G = 300 W/m^2$).

4.5. The impact of PV/T collector area

The PV/T collector area directly affects the solar input value and electrical output of the PV. In both cases, larger PV/T collector areas can enhance the system efficiency and reduction of the grid. In order to show the impact of PV/T collector area for two different ambient temperatures, Fig. 12 is given including ejector and PV contributions. Increment of the collector area has a positive effect on system performance and on

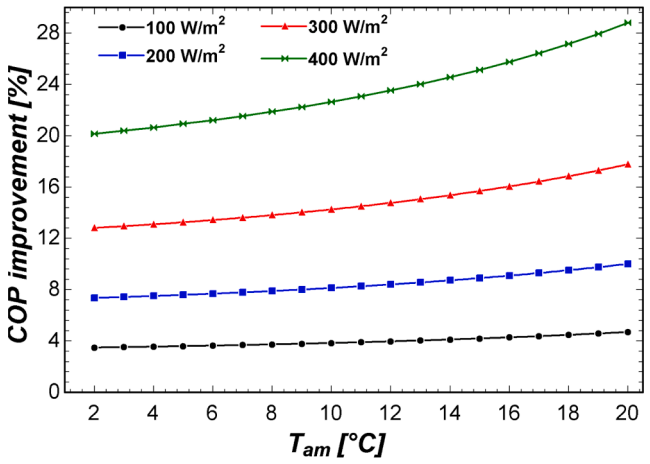

Fig. 11. COP improvement by using optimum PV/T evaporator temperature by ambient temperature.

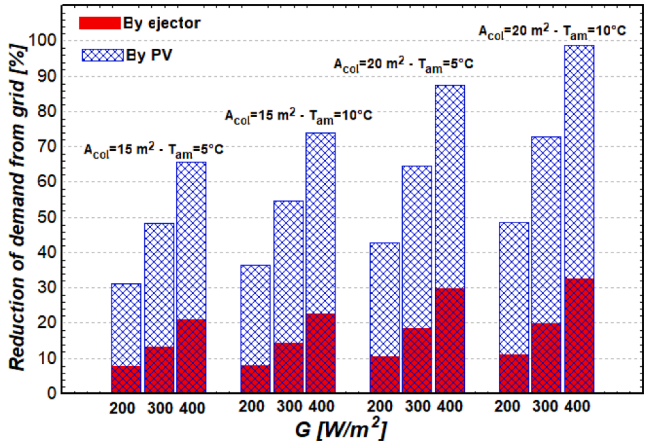

Fig. 12. Reduction from the grid according to ejector and PV output contributions for different collector areas and ambient temperatures.

reduction of grid demand. In this figure, the effect of the ambient temperature can be seen clearly because electricity consumption reduces even for conventional heat pumps in higher ambient temperatures. By using a PV/T collector with an area of 20 m^2 for an ambient temperature of 10 °C and a solar irradiance of 400 W/m^2, electricity demand reduction from the grid can be maintained about 32.5 % by ejector and 98 % in overall.

4.6. The impact of refrigerant type

As the refrigerant used has an influence on the operation conditions and system performance, the impact of other low global warming potential refrigerants is investigated. The effect of the refrigerant types on the COP improvement is given in Fig. 13 for different PV/T collector evaporation temperatures (T_m) for the refrigerants R1234yf, R290, R717, and R1234ze(E). The results are obtained for 5 °C ambient temperature 300W/m^2 solar irradiance. The properties of these refrigerants can be found in reference [53]. The highest COP improvements are obtained around $T_m = 10$°C for all the working fluids considered. The improvement of the R1234yf and R1234ze(E) are close to each other. The lowest improvement is obtained for R290 and the highest for R717.

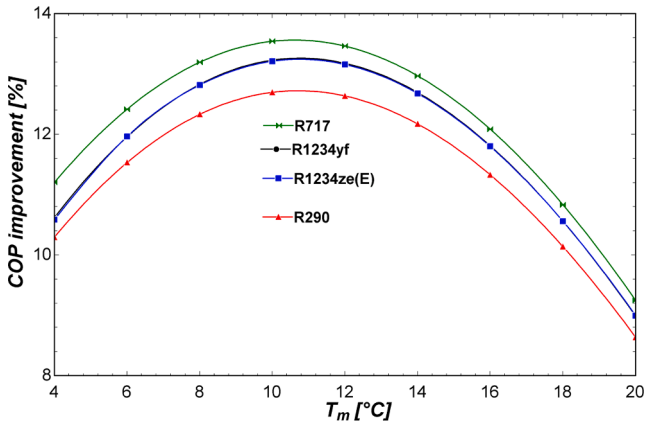

Fig. 13. Effect of the refrigerant type on COP improvement for different PV/T collector evaporation temperatures (T_m).

4.7. COP improvement and demand reduction potentials over one month period in two selected cities

After investigating the effect of the operation parameters on performance, the system performance is analysed by using real weather conditions. Previously given weather data of the two cities are used to calculate COP improvement and reduction percentages from the grid for a one-month period. Fig. 14a shows the comparison of two cities' COP improvement potentials. By operating the system for 7 h in a day which represents office working hours and higher than 100 W/m^2 solar irradiance for 15 m^2 PV/T collectors. The COP improvement for the coldest month in Adana and Istanbul can reach up to 25.5 % and 30 %, respectively. However, the average COP improvement in Adana is calculated about 14 % and in Istanbul, it is about 8.5 %. Fig. 14b shows the demand reduction, for the two cities. The average values are calculated as 61.08 % for Adana and 40.4 % for Istanbul. These promising results were calculated for the coldest months; however, heat

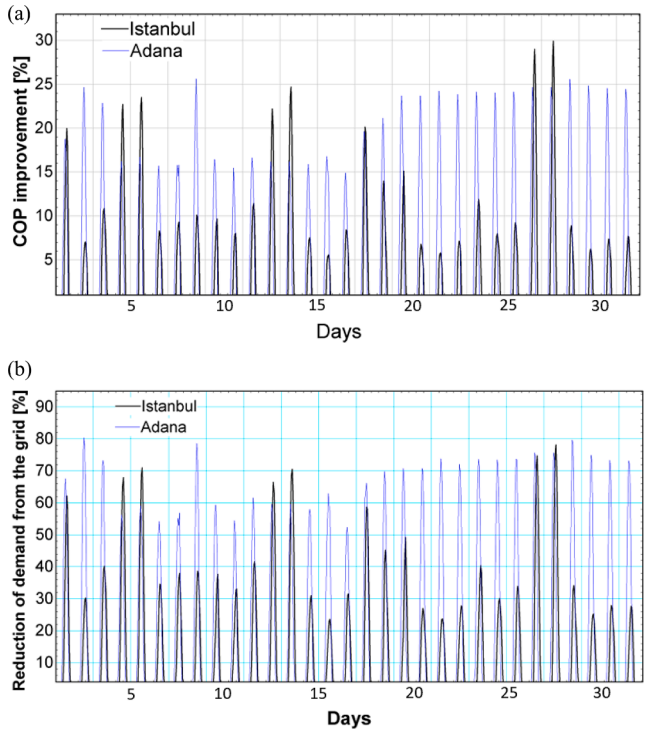

Fig. 14. A) COP improvement by ejector enhanced unit (PV/T area = 15 m^2) **b)** Reduction of demand from the grid including PV output (PV/T area = 15 m^2).

pumps are used in all heating seasons. For example, in March, the weather temperature and solar irradiance will be higher which will generate more PV output, and less compressor consumption due to higher air evaporator temperature. Also, better weather conditions mean better ejector contribution resulting in higher COP improvement potential. Moreover, after the heating season, the PV can continue to produce electricity in summer. Considering the given advantages, payback time of the system will be shorter.

5. Conclusions

In this study, performance improvement potential of the conventional air sourced heat pump unit has been promoted by using a solar heat source and an ejector. The unit operates under two different temperatures of heat sources, solar and air sources. The ejector has increased the low evaporation pressure before entering the compressor by using relatively higher-pressured refrigerant stream from the solar collector line. The system performance has been improved by choosing an optimum solar collector operation temperature according to the used PV/T collector performance. Additionally, electricity generation from the PV/T collector reduced the demand for electricity from the grid. In this way, utilization of solar energy would make a positive impact on environmental issues. The parameters affecting the performance have been investigated and the following conclusions can be drawn:

- The proposed design overcomes the dependency of the solar profile of the direct expansion solar-assisted heat pumps which causes limited heating capacity in low solar radiation days, however, this unit can operate smoothly as a conventional heat pump even without solar radiation.
- The solar heat input has a positive effect on performance in two ways. Firstly, it increases the enthalpy of the ejector inlet, and resulting in better ejector performance. Secondly, higher solar inputs reduce the low-pressure refrigerant flow rate which also helps to increase the pressure lift and COP.
- The solar collector evaporation pressure has an optimum operating temperature to maximise benefit from the solar input and ejector operation.
- The COP of the heat pump can be improved by 22.6 % over common vapour compression heat pump technologies depending on the solar irradiance level and ambient temperature when using a PV/T collector of 15 m^2.
- The consumed electricity from the grid can be reduced by 75 % when considering the generated electricity from the PV when using a 15 m^2 PV/T collector.

Declaration of Competing Interest

The authors declare that they have no known competing financial interests or personal relationships that could have appeared to influence the work reported in this paper.

Data availability

No data was used for the research described in the article.

Acknowledgment

O. Aydin acknowledges the partial support by the Turkish Academy of Sciences.

References

[1] Enhancing Turkey's policy framework for energy efficiency of buildings, and recommendations for the way forward based on international experiences, 2019.
[2] K.J. Chua, S.K. Chou, W.M. Yang, Advances in heat pump systems: A review, Appl. Energy. (2010), https://doi.org/10.1016/j.apenergy.2010.06.014.
[3] R. Yumrutas, Ö. Kaşka, Experimental investigation of thermal performance of a solar assisted heat pump system with an energy storage, Int. J. Energy Res. 28 (2004) 163–175, https://doi.org/10.1002/er.959.
[4] J.G. Cervantes, E. Torres-Reyes, Experiments on a solar-assisted heat pump and an exergy analysis of the system, Appl. Therm. Eng. 22 (2002) 1289–1297, https://doi.org/10.1016/S1359-4311(02)00055-8.
[5] M.S. Buker, S.B. Riffat, Solar assisted heat pump systems for low temperature water heating applications: A systematic review, Renew. Sustain. Energy Rev. 55 (2016) 399–413, https://doi.org/10.1016/j.rser.2015.10.157.
[6] J. Ji, G. Pei, T.-T. Chow, K. Liu, H. He, J. Lu, C. Han, Experimental study of photovoltaic solar assisted heat pump system, Sol. Energy. 82 (1) (2008) 43–52.
[7] X. Kong, P. Sun, S. Dong, K. Jiang, Y. Li, Experimental performance analysis of a direct-expansion solar-assisted heat pump water heater with R134a in summer, Int. J. Refrig. 91 (2018) 12–19, https://doi.org/10.1016/j.ijrefrig.2018.04.021.
[8] R.M. Lazzarin, Dual source heat pump systems: Operation and performance, Energy Build. 52 (2012) 77–85, https://doi.org/10.1016/j.enbuild.2012.05.026.
[9] B. Du, Z. Quan, L. Hou, Y. Zhao, X. Lou, C. Wang, Experimental study on the performance of a photovoltaic/thermal-air dual heat source direct-expansion heat pump, Appl. Therm. Eng. 188 (2021), 116598, https://doi.org/10.1016/j.applthermaleng.2021.116598.
[10] B. Buonomo, A. di Pasqua, O. Manca, S. Nardini, Evaluation of thermal and fluid dynamic performance parameters in aluminum foam compact heat exchangers, Appl. Therm. Eng. 176 (2020), 115456, https://doi.org/10.1016/j.applthermaleng.2020.115456.
[11] J. Cai, Z. Li, J. Ji, F. Zhou, Performance analysis of a novel air source hybrid solar assisted heat pump, Renew. Energy. 139 (2019) 1133–1145, https://doi.org/10.1016/j.renene.2019.02.134.
[12] C. Bai, Z. Han, H. Wei, X. Ju, X. Meng, Q. Fu, Simulation study on performance of a dual-source hybrid heat pump unit with alternative refrigerants, Energy, Built Environ. 1 (2020) 1–10, https://doi.org/10.1016/j.enbenv.2019.08.004.
[13] X. Li, Y. Wang, M. Li, M. Hang, W. Zhao, D. Kong, G. Yin, Performance testing of a heat pump system with auxiliary hot water under different ambient temperatures, Energy Built Environ. (2021), https://doi.org/10.1016/j.enbenv.2021.02.002.
[14] I. Grossi, M. Dongellini, A. Piazzi, G.L. Morini, Dynamic modelling and energy performance analysis of an innovative dual-source heat pump system, Appl. Therm. Eng. 142 (2018) 745–759, https://doi.org/10.1016/j.applthermaleng.2018.07.022.
[15] Z. Han, X. Ju, L. Qu, J. Liu, X. Ma, S. Zhang, Experimental study of the performance of a double-source heat-pipe composite vapour-compression heating unit, Sol. Energy. 155 (2017) 1208–1215, https://doi.org/10.1016/j.solener.2017.07.062.
[16] Y. Liu, J. Ma, G. Zhou, C. Zhang, W. Wan, Performance of a solar air composite heat source heat pump system, Renew. Energy. 87 (2016) 1053–1058, https://doi.org/10.1016/j.renene.2015.09.001.
[17] J. Cai, H. Zhou, L. Xu, T. Zhang, Experimental and numerical investigation on the heating performance of a novel multi-functional heat pump system with solar-air composite heat source, Sustain. Cities Soc. (2021), https://doi.org/10.1016/j.scs.2021.103118.
[18] Z. Liu, Q. Wang, D. Wu, Y. Zhang, H. Yin, H. Yu, G. Jin, X. Zhao, Operating performance of a solar/air-dual source heat pump system under various refrigerant flow rates and distributions, Appl. Therm. Eng. 178 (2020), https://doi.org/10.1016/j.applthermaleng.2020.115631.
[19] G. Pei, J. Ji, C. Han, W. Fan, Performance of solar assisted heat pump using PV evaporator under different compressor frequency, ISES Sol. World Congr. 2007, ISES 2007. 2 (2007) 935–939. 10.1007/978-3-540-75997-3_180.
[20] J. Cai, J. Ji, Y. Wang, F. Zhou, B. Yu, A novel PV/T-air dual source heat pump water heater system: Dynamic simulation and performance characterization, Energy Convers. Manag. 148 (2017) 635–645, https://doi.org/10.1016/j.enconman.2017.06.036.
[21] Ş. Ünal, M.T. Erdinç, Ç. Kutlu, Optimal thermodynamic parameters of two-phase ejector refrigeration system for buses, Appl. Therm. Eng. 124 (2017) 1354–1367, https://doi.org/10.1016/j.applthermaleng.2017.06.115.
[22] J. Chen, J. Yu, Theoretical analysis on a new direct expansion solar assisted ejector-compression heat pump cycle for water heater, Sol. Energy. 142 (2017) 299–307, https://doi.org/10.1016/j.solener.2016.12.043.
[23] A. Zarei, S. Elahi, H. Pahangeh, Design and analysis of a novel solar compression-ejector cooling system with eco-friendly refrigerants using hybrid photovoltaic thermal (PVT) collector, Therm. Sci. Eng. Prog. 32 (2022), 101311, https://doi.org/10.1016/j.tsep.2022.101311.
[24] Ş. Ünal, E. Cihan, M.T. Erdinç, M. Bilgili, Influence of mixing section inlet and diffuser outlet velocities on the performance of ejector-expansion refrigeration system using zeotropic mixture, Therm. Sci. Eng. Prog. 33 (2022), https://doi.org/10.1016/j.tsep.2022.101338.
[25] Ü. İşkan, M. Direk, Evaluation of the effects of entrainment ratios on the performance parameters of a refrigeration machine having dual evaporator ejector system with R134a and R456A, Therm. Sci. Eng. Prog. 33 (2022), https://doi.org/10.1016/j.tsep.2022.101345.
[26] S. Li, J. Lu, J. Yan, Y. Hu, Performance analysis of auxiliary entrainment ejector used in multi-evaporator refrigeration system, Therm. Sci. Eng. Prog. 32 (2022), 101307, https://doi.org/10.1016/j.tsep.2022.101307.
[27] G. Besagni, R. Mereu, F. Inzoli, Ejector refrigeration: A comprehensive review, Renew. Sustain. Energy Rev. 53 (2016) 373–407, https://doi.org/10.1016/j.rser.2015.08.059.
[28] G. Besagni, R. Mereu, G. Di Leo, F. Inzoli, A study of working fluids for heat driven ejector refrigeration using lumped parameter models, Int. J. Refrig. 58 (2015) 154–171, https://doi.org/10.1016/j.ijrefrig.2015.06.015.

[29] C. Lin, Y. Li, W. Cai, J. Yan, Y. Hu, Experimental investigation of the adjustable ejector in a multi-evaporator refrigeration system, Appl. Therm. Eng. 61 (2013) 2–10, https://doi.org/10.1016/j.applthermaleng.2013.07.045.
[30] A. Khalid Shaker Al-Sayyab, A. Mota-Babiloni, J. Navarro-Esbrí, Novel compound waste heat-solar driven ejector-compression heat pump for simultaneous cooling and heating using environmentally friendly refrigerants, Energy Convers. Manag. 228 (2021). 10.1016/j.enconman.2020.113703.
[31] C. Fan, G. Yan, J. Yu, Thermodynamic analysis of a modified solar assisted ejector-compression heat pump cycle with zeotropic mixture R290/R600a, Appl. Therm. Eng. 150 (2019) 42–49, https://doi.org/10.1016/j.applthermaleng.2019.01.011.
[32] F. Li, Z. Chang, X. Li, Q. Tian, Energy and exergy analyses of a solar-driven ejector-cascade heat pump cycle, Energy. 165 (2018) 419–431, https://doi.org/10.1016/j.energy.2018.09.173.
[33] G. Yan, T. Bai, J. Yu, Energy and exergy efficiency analysis of solar driven ejector-compressor heat pump cycle, Sol. Energy. 125 (2016) 243–255, https://doi.org/10.1016/j.solener.2015.12.021.
[34] J. Liu, Z. Lin, Thermodynamic analysis of a novel dual-temperature air-source heat pump combined ejector with zeotropic mixture R1270/R600a, Energy Convers. Manag. 220 (2020), 113078, https://doi.org/10.1016/j.enconman.2020.113078.
[35] J. Liu, Z. Lin, A novel dual-temperature ejector-compression heat pump cycle - exergetic and economic analyses, Int. J. Refrig. 126 (2021) 155–167, https://doi.org/10.1016/j.ijrefrig.2021.01.005.
[36] M. Wang, Y. Cheng, J. Yu, Analysis of a dual-temperature air source heat pump cycle with an ejector, Appl. Therm. Eng. 193 (2021), 116994, https://doi.org/10.1016/j.applthermaleng.2021.116994.
[37] L. Zhu, J. Yu, M. Zhou, X. Wang, Performance analysis of a novel dual-nozzle ejector enhanced cycle for solar assisted air-source heat pump systems, Renew. Energy. 63 (2014) 735–740, https://doi.org/10.1016/j.renene.2013.10.030.
[38] D.W. Sun, Variable geometry ejectors and their applications in ejector refrigeration systems, Energy. 21 (1996) 919–929, https://doi.org/10.1016/0360-5442(96)00038-2.
[39] S. Varga, P.M.S. Lebre, A.C. Oliveira, CFD study of a variable area ratio ejector using R600a and R152a refrigerants, Int. J. Refrig. 36 (2013) 157–165, https://doi.org/10.1016/j.ijrefrig.2012.10.016.
[40] C. Li, Y. Li, W. Cai, Y. Hu, H. Chen, J. Yan, Analysis on performance characteristics of ejector with variable area-ratio for multi-evaporator refrigeration system based on experimental data, Appl. Therm. Eng. 68 (2014) 125–132, https://doi.org/10.1016/j.applthermaleng.2014.04.031.
[41] C. Li, J. Yan, Y. Li, W. Cai, C. Lin, H. Chen, Experimental study on a multi-evaporator refrigeration system with variable area ratio ejector, Appl. Therm. Eng. 102 (2016) 196–203, https://doi.org/10.1016/j.applthermaleng.2016.04.006.
[42] S. Li, J. Yan, Z. Liu, Y. Yao, X. Li, N. Wen, G. Zou, Optimization on crucial ejector geometries in a multi-evaporator refrigeration system for tropical region refrigerated trucks, Energy. 189 (2019), 116347, https://doi.org/10.1016/j.energy.2019.116347.
[43] A. Yilmaz, Transcritical organic Rankine vapor compression refrigeration system for intercity bus air-conditioning using engine exhaust heat, Energy. 82 (2015) 1047–1056, https://doi.org/10.1016/j.energy.2015.02.004.
[44] O. Brunin, M. Feidt, B. Hivet, Comparison of the working domains of some compression heat pumps and a compression-absorption heat pump, Int. J. Refrig. 20 (1997) 308–318, https://doi.org/10.1016/S0140-7007(97)00025-X.
[45] S. Bhattarai, J. Oh, S. Euh, G. Krishna, D. Hyun, Solar Energy Materials & Solar Cells Simulation and model validation of sheet and tube type photovoltaic thermal solar system and conventional solar collecting system in transient states, Sol. Energy Mater. Sol. Cells. 103 (2012) 184–193, https://doi.org/10.1016/j.solmat.2012.04.017.
[46] D. Gao, J. Li, X. Ren, T. Hu, G. Pei, A novel direct steam generation system based on the high-vacuum insulated flat plate solar collector, Renew. Energy. 197 (2022) 966–977, https://doi.org/10.1016/j.renene.2022.07.102.
[47] Ş. Ünal, T. Yilmaz, Thermodynamic analysis of the two-phase ejector air-conditioning system for buses, Appl. Therm. Eng. 79 (2015) 108–116, https://doi.org/10.1016/j.applthermaleng.2015.01.023.
[48] National Renewable Energy Laboratory (NREL), EnergyPlus Weather Data, EnergyPlus. (2019). https://energyplus.net/.
[49] J. Yan, S. Li, Z. Liu, Numerical investigation on optimization of ejector primary nozzle geometries with fixed/varied nozzle exit position, Appl. Therm. Eng. 175 (2020), 115426, https://doi.org/10.1016/j.applthermaleng.2020.115426.
[50] A.K.S. Al-Sayyab, J. Navarro-Esbrí, V.M. Soto-Francés, A. Mota-Babiloni, Conventional and Advanced Exergoeconomic Analysis of a Compound Ejector-Heat Pump for Simultaneous Cooling and Heating, Energies. 14 (2021) 3511, https://doi.org/10.3390/en14123511.
[51] H. Wen, J. Yan, Effect of mixing chamber length on ejector performance with fixed / varied area ratio under three operating conditions in refrigerated trucks, Appl. Therm. Eng. 197 (2021), 117379, https://doi.org/10.1016/j.applthermaleng.2021.117379.
[52] Y. Jeon, H. Kim, J.H. Ahn, S. Kim, Effects of nozzle exit position on condenser outlet split ejector-based R600a household refrigeration cycle, Energies. 13 (2020), https://doi.org/10.3390/en13195160.
[53] D. Wu, B. Hu, R.Z. Wang, Vapor compression heat pumps with pure Low-GWP refrigerants, Renew. Sustain. Energy Rev. 138 (2021), https://doi.org/10.1016/j.rser.2020.110571.